Inorg. Chem. **1986**, *25*, 4507–4514

Contribution from the Division of Chemical and Physical Sciences, Deakin University, Waurn Ponds 3217, Victoria, Australia, and Department of Chemistry, Faculty of Education, Mie University, Kamihama, Tsu, Mie 514, Japan

Spectrophotometric and Voltammetric Characterization of Complexes of Bis(2,2′-bipyridine)(2,2′-bibenzimidazole)ruthenium and -osmium in Oxidation States II, III, and IV in Acetonitrile–Water Mixtures

Alan M. Bond*[1] and Masa-aki Haga*[2,3]

Received April 25, 1986

A combination of spectrophotometric and voltammetric studies has enabled a complete description of the acid–base and redox chemistry of $[M(bpy)_2(BiBzImH_2)]^{2+}$ complexes to be provided in a 50% acetonitrile–water medium in each of the oxidation states II, III, and IV (M = Ru, Os; bpy = 2,2′-bipyridine; $BiBzImH_2$ = 2,2′-bibenzimidazole). Over the pH range 0–12 nonprotonated, monoprotonated and diprotonated M(II) and M(III) complexes can be identified (protonation is associated with the imidazole ligand) whereas for M(IV) complexes protonation does not occur even at pH 0. Calculated pK_a values show that the acid strength increases markedly with increase in oxidation state. In the redox sense, osmium(III) and osmium(IV) complexes are more accessible via oxidation of osmium(II) than are their ruthenium analogues. At no pH value in the range 0–12 does a crossover of the order of reversible half-wave potentials for the M(III)/M(II) and M(IV)/M(III) redox couples occur so that stabilization of oxidation state III complexes with respect to disproportionation is achieved. The osmium(III) complexes are readily prepared electrochemically as stable entities in acetonitrile/water mixtures whereas the ruthenium(III) complexes are comparatively reactive. The presence of the imidazole ligand stabilizes the oxidation state IV complexes of ruthenium and osmium so that they can be observed under fast scan rate conditions (>5 V s^{-1}) with cyclic voltammetry or with short pulse widths (<10 ms) with differential pulse voltammetry at glassy carbon electrodes. With longer time scale voltammetric experiments a chemically irreversible catalytic process is observed. The potential range available at glassy-carbon electrodes, but not at platinum, is adequate to observe the M(III)/M(IV) oxidation process prior to onset of oxidation of water. Comparison with the acid–base and redox behavior of related systems reveals interesting differences. For example the similarity in pH dependence of the two metals leads to the conclusion that both oxidation processes are metal based, in contrast to other studies on $[M(bpy)_3]^{2+}$ where it has been suggested that the second process is metal based for osmium but ligand based for ruthenium.

Introduction

Nitrogen ligands coordinated to ruthenium and osmium as well other metals have been studied extensively,[4] and it has been demonstrated that many nitrogen ligands exhibit well-defined acid–base properties in aqueous media, which can be modified by coordination to a metal. For example, Hoq and Shepherd have described in detail the influence of different metal centers on the pK_a of the pyrrole hydrogen of imidazole complexes of $(NH_3)_5M^{3+}$ (M = Co(III), Rh(III), Ir(III), Ru(III)).[5] The pK_a value is a function of the d^n configuration of the metal and other related parameters.[5]

As an alternative to varying the metal center, the oxidation state of the metal can be systematically altered by oxidation and/or reduction and the variation in pK_a of coordinated ligand assessed as function of oxidation state. In the particular case of ruthenium and osmium, common oxidation states are II and III. Acid–base properties of nitrogen ligands coordinated to M(II) and M(III) (M = Ru, Os) have been reported.[6] Ruthenium(IV) and osmium(IV) complexes are relatively rare with only a few well-characterized complexes being known,[7] and information on their acid–base chemistry is sparse. Taube et al. have measured the pK_a values for a series of $[Os(NH_3)_xX_{6-x}]^{n+}$ (x = 4 or 3) complexes.[8] The comparison of pK_a values for $[Os(NH_3)_6]^{3+}$ and $[Os(NH_3)_6]^{4+}$ demonstrated an extremely strong dependence on oxidation state.[8,9] In some reactions of coordinated ligands such as oxidative dehydrogenation, a Ru(IV) intermediate has been regarded as a key compound.[10]

Complexes of the kind bis(2,2′-bipyridine)(2,2′-bibenzimidazole)metal(2+) (metal = Ru, Os), $[M(bpy)_2(BiBzImH_2)]^{2+}$, can be prepared[11] in oxidation state II (structure I). In the $BiBzImH_2$ ligand, clearly there are two protons that can exhibit acid–base properties.

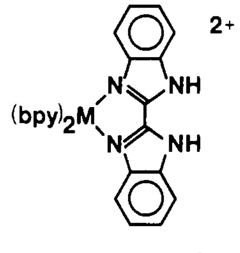

M = Ru and Os

I

Electrochemical oxidation of oxidation state II complexes of this kind may be expected to produce oxidation state III complexes. Oxidation state IV may be accessible prior to oxidation of water. In this work, electrochemical studies have been undertaken to ascertain whether higher oxidation state complexes of I are accessible, and if so, what form the complexes are in with respect to the acid–base properties of the ligand. Studies in aqueous media are precluded because of low solubility of complex I at higher pH. Consequently, 50% water/acetonitrile was chosen as the medium for both spectrophotometric and electrochemical investigations aimed at identifying the nature of the species present in each oxidation state.

---

(1) Deakin University.

(2) Mie University.

(3) On leave at Deakin University, Sept 1985 to Sept 1986.

(4) (a) Kalyanasundaram, K. *Coord. Chem. Rev.* **1982**, *46*, 159. (b) Seddon, E. A.; Seddon, K. R. *The Chemistry of Ruthenium*; Elsevier: Amsterdam, 1984. (c) Griffith, W. P. *The Chemistry of the Rarer Platinum Metals*; Wiley-Interscience: New York, 1967.

(5) (a) Hoq, M. F.; Shepherd, R. E. *Inorg. Chem.* **1984**, *23*, 1851. (b) Johnson, C. R.; Henderson, W. W.; Shepherd, R. E. *Inorg. Chem.* **1984**, *23*, 2754.

(6) (a) Ford, P.; Rudd, D. F. P.; Gaunder, R.; Taube, H. *J. Am. Chem. Soc.* **1968**, *90*, 1187. (b) Lavallee, D. K.; Fleischer, E. B. *J. Am. Chem. Soc.* **1972**, *94*, 2583. (c) Crutchley, R. J.; Kress, N.; Lever, A. B. P. *J. Am. Chem. Soc.* **1983**, *105*, 1170. (d) Clarke, M. J. *J. Am. Chem. Soc.* **1978**, *100*, 5068. (e) Toma, H. E.; Stadler, E. *Inorg. Chem.* **1985**, *24*, 3085 and references cited therein. (f) Sundberg, R. J.; Bryan, R. F.; Taylor, I. F.; Taube, H. *J. Am. Chem. Soc.* **1974**, *96*, 381.

(7) (a) Bailer, J. C.; Emelius, H. J.; Nyholm, R.; Trotman-Dickenson, A. F. *Comprehensive Inorganic Chemistry*, 1st ed.; Pergamon: New York, 1973; Vol. 3, p 1207. (b) Cotton, F. A.; Wilkinson, G. *Advanced Inorganic Chemistry*, 4th Ed.; Wiley: New York, 1980; p 912. (c) Bhattacharya, S.; Chakravarty, A.; Cotton, F. A.; Mukherjee, R.; Schwotzer, W. *Inorg. Chem.* **1984**, *23*, 1709 and references cited therein.

(8) Buhr, J. D.; Winkler, J. R.; Taube, H. *Inorg. Chem.* **1980**, *19*, 2416.

(9) Bottomley, F.; Tong, S. B. *Inorg. Chem.* **1974**, *13*, 243.

(10) Ridd, M. J.; Keene, F. R. *J. Am. Chem. Soc.* **1981**, *103*, 5733 and references cited therein.

(11) Haga, M. *Inorg. Chim. Acta* **1983**, *75*, 29.

0020-1669/86/1325-4507$01.50/0 © 1986 American Chemical Society

Experimental Section

Materials. 2,2′-Bibenzimidazole ($BiBzImH_2$)[12] and $[Ru^{II}(bpy)_2(BiBzImH_2)](ClO_4)_2$[11] were prepared by literature methods. A sample of $Os(bpy)_2Cl_2$ was kindly donated by Professor Takeko Matsumura-Inoue at Nara University of Education, Japan. The water used in spectrophotometric and electrochemical measurements was deionized and then distilled. Acetonitrile was of HPLC grade and used without further purification. All other chemicals were of analytical grade.

Buffer systems and the pH ranges employed were as follows:[13] pH 0–2, $HClO_4$ and $NaClO_4$; pH 2–4, phthalate; pH 4–8, phosphate; pH 8–11, borate.

Synthesis. $[Os^{II}(bpy)_2(BiBzImH_2)](ClO_4)_2 \cdot 3H_2O$. A suspended mixture of $Os(bpy)_2Cl_2$ (0.3 g, 0.5 mmol) and $BiBzImH_2$ (0.23 g, 1.0 mmol) was heated under refluxing conditions for 40 h in ethanol/water (1:1 v/v, 70 cm^3), during which time the color changed from dark violet to dark yellow. The resulting solution was evaporated under reduced pressure to half the initial volume and then filtered. To the filtrate was added sodium perchlorate (0.30 g, 2.1 mmol), and the solution was chilled in a refrigerator. The solid was collected by filtration and recrystallized from methanol in 80% yield. Anal: Calcd for $C_{34}H_{26}N_8O_8ClOs \cdot 3H_2O$: C, 41.26; H, 3.26; N, 11.32. Found: C, 41.11; H, 2.95; N, 11.34.

Physical Measurements. Electronic spectra were recorded on a Hitachi U-3200 spectrophotometer using 1-cm matched quartz cells. The pH measurements were made with a Metrohm Model E512 pH meter standardized with standard buffers of pH 4.0, 7.0, and 9.0. As the pH meter responds in a reproducible way to hydrogen ions in a 50% acetonitrile–water mixture,[13] the "apparent" pH values of this mixture have been determined directly from the meter reading. Unless otherwise stated, the "apparent" pH values are referred to as pH. Spectrophotometric titrations were performed in acetonitrile/water (1:1 v/v) solution. The solution was deaerated by a steady argon bubbling and titrated with a 0.01 mol dm^{-3} NaOH or HCl aqueous solution. The pK_a values of the deprotonation in the complexes were calculated by using the equation

$$\mathrm{pH} = \mathrm{p}K_a - \log \frac{[\mathrm{acid}]}{[\mathrm{base}]} = \mathrm{p}K_a - \log \frac{A - A_0}{A_f - A}$$

where A_0 and A_f are the initial and final absorbances, respectively. Some A_0 and A_f values were evaluated from the graphical method of Coleman et al.,[14] because two closely spaced deprotonation equilibria exist in this system.

Electrochemical measurements were made at 25 °C with either a Bioanalytical Systems BAS-100 Electrochemical Analyzer or a Princeton Applied Research Corp. (PARC) Model 174 Polarographic Analyzer equipped with a Houston Model 2000 X-Y recorder. The working electrodes were glassy-carbon or platinum disk electrodes and the auxiliary electrode was a platinum wire. The wider positive potential range available on the glassy-carbon electrode made this the electrode of choice for studies of oxidation state IV complexes and unless otherwise stated this working electrode material was used rather than platinum. The glassy-carbon working disk electrode was frequently polished with an alumina/water slurry. This cleaning procedure is essential to obtain reproducible results for the studies of higher oxidation states. The reference electrode, separated from the cell by a salt bridge, was Ag/AgCl (acetone, saturated with dry LiCl). The ferrocene–ferrocenium (Fc/Fc^+) redox couple was measured to provide an internal reference[15] during the same electrochemical experiment, and all potentials were referred to those for Fc/Fc^+ couple. In the same solvent system, the $E^r_{1/2}$ value ($E^r_{1/2}$ = reversible half-wave potential) for oxidation of $[Ru(bpy)_3](ClO_4)_2$ is +0.916 V vs. Fc/Fc^+ at pH 7.

Controlled-potential electrolysis experiments were carried out at a platinum-gauze working electrode, with the use of a PARC 173/179 potentiostat/digital coulometer. The reference electrode was the same Ag/AgCl electrode used in voltammetric experiments, and the auxiliary electrode was platinum gauze separated from the test solution by a salt bridge containing the solvent mixture. All solutions were degassed with nitrogen prior to undertaking electrochemical experiments.

Results and Discussion

The oxidation chemistry of osmium is presented first because of the greater stability of higher oxidation state complexes. The high oxidation state ruthenium complexes are relatively reactive and some of the interpretations for the ruthenium metal complex are based on analogy with osmium data.

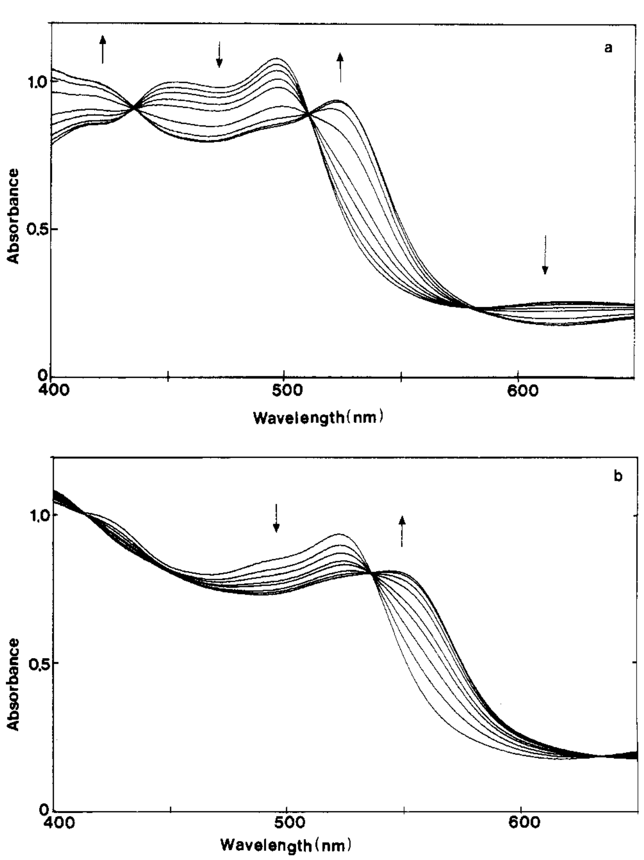

Figure 1. Absorption spectra of $[Os^{II}(bpy)_2(BiBzImH_2)](ClO_4)_2$ (9.4 × 10^{-5} mol dm^{-3}) at 25 °C in CH_3CN/buffer (1:1 v/v) at various pH: (a) lower pH region, pH 3.15, 3.92, 4.35, 4.72, 4.96, 5.52, 6.10, 7.19, and 8.20; (b) higher pH region, pH 8.20, 9.05, 9.47, 9.78, 9.98, 10.34, 10.71, 11.28, and 11.52.

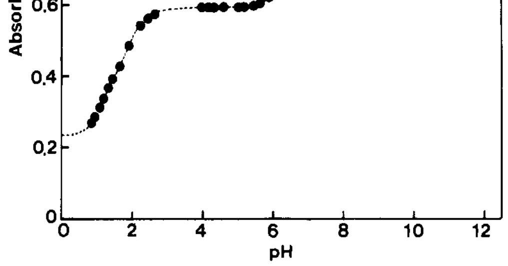

Figure 2. Spectrophotometric titration curves in CH_3CN/buffer (1:1 v/v) of (a) $[Os^{II}(bpy)_2(BiBzImH_2)]^{2+}$ at 500 nm and (b) $[Os^{III}(bpy)_2(BiBzImH_2)]^{3+}$ generated chemically in situ at 610 nm. Temperature = 25 °C.

$[Os(bpy)_2(BiBzImH_2)](ClO_4)_2$. Spectrophotometric Studies on Osmium(II). The $[Os^{II}(bpy)_2(BiBzImH_2)]^{2+}$ complex at pH <3 has a strong absorption band at 497 nm, which can be assigned to a metal-to-ligand charge-transfer (MLCT) band.[16] As the

---

[12] Fieselmann, B. F.; Hendrickson, D. N.; Stucky, G. D. *Inorg. Chem.* **1978**, *17*, 2078.

[13] Perrin, D. D.; Dempsey, B. *Buffers for pH and Metal Ion Control*; Chapman & Hall: London, 1974.

[14] Coleman, J. S.; Varga, L. P.; Mastin, S. H. *Inorg. Chem.* **1970**, *9*, 1015.

[15] Gagne, R. R.; Koval, C. A.; Lisensky, G. C. *Inorg. Chem.* **1980**, *19*, 2854.

[16] Kober, E. M.; Meyer, T. J. *Inorg. Chem.* **1982**, *21*, 3967.

Table I. Cyclic Voltammetric Data in CH_3CN/buffer (1:1 v/v) at 25 °C for the First Oxidation Process for $[M(bpy)_2(BiBzImH_2)](ClO_4)_2$ Obtained at Various pH Values by Using a Glassy-Carbon Electrode[a]

	M = Ru				M = Os			
pH	E^{ox}_p, V vs. Fc/Fc$^+$	ΔE_p, mV	$E^r_{1/2}$, V vs. Fc/Fc$^+$	i^{ox}_p/i^{red}_p	E^{ox}_p, V vs. Fc/Fc$^+$	ΔE_p, mV	$E^r_{1/2}$, V vs. Fc/Fc$^+$	i^{ox}_p/i^{red}_p
1.10	+0.727	65	+0.695	1.15	+0.311	60	+0.283	1.07
2.10	+0.674	67	+0.640	1.08	+0.264	67	+0.230	0.99
3.60	+0.591	65	+0.559	0.98	+0.206	60	+0.176	0.97
4.61					+0.144	73	+0.108	1.00
5.30	+0.513	62	+0.483	1.05	+0.104	80	+0.071	1.00
6.83	+0.436	65	+0.403	1.12	+0.050	63	+0.019	1.00
7.83	+0.376	65	+0.344	1.10	−0.013	67	−0.047	1.06
9.35	+0.290	58	+0.261	1.13	−0.079	77	−0.117	1.06
10.56	+0.242	58	+0.214	1.05	−0.091	80	−0.131	1.00
11.32	+0.242	68	+0.208	1.05				
12.65	+0.238	62	+0.207	1.12	−0.107	64	−0.137	1.06

[a] E^{ox}_p = peak potential for oxidation, ΔE_p = peak separation for oxidation and reduction, $E^r_{1/2}$ = calculated reversible half-wave potential, i^{ox}_p = peak current for oxidation, and i^{red}_p = peak current for reduction.

pH of a solution of $[Os^{II}(bpy)_2(BiBzImH_2)]^{2+}$ is raised, this band shifts to 522 nm and finally 548 nm with a decrease in intensity. Figure 1a shows absorption spectra of $[Os^{II}(bpy)_2(BiBzImH_2)](ClO_4)_2$ as a function of pH in the low pH region. Three well-defined isosbestic points at 435, 510, and 519 nm can be seen. Figure 1b shows equivalent data at high pH with three isosbestic points at 414, 536, and 635 nm again being present. The osmium(II) complex is stable at all pH values examined, and stepwise acid–base equilibria are involved. Figure 2 shows the titration curve obtained at 500 nm. The equilibria are shown in eq 1, where BiBzImH and BiBzIm were used as abbreviations

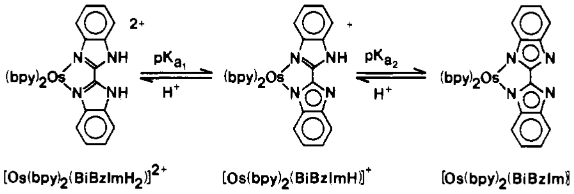

(1)

for mono- and di-deprotonated forms of $BiBzImH_2$, respectively. The calculated values of pK_{a_1} and pK_{a_2} are 5.08 ± 0.05 and 9.59 ± 0.05 at 25 °C.

Spectrophotometric Studies on Osmium(III). Electrochemical data (see later) demonstrate that oxidation to osmium(III) occurs at about +0.2 V vs. Fc/Fc$^+$ at pH 2 while the oxidation state IV is achieved at about +1.1 V vs. Fc/Fc$^+$. $NOBF_4$ was found to be an ideal chemical oxidant to quantitatively produce the osmium(III) oxidation state.

The osmium(III) species generated chemically are identical with those formed by controlled-potential electrolysis at +0.6 V vs. Fc/Fc$^+$.

The visible spectra of $[Os^{III}(bpy)_2(BiBzImH_2)]^{3+}$ at pH 1 exhibit weak broad bands at around 520 nm, which can be assigned to ligand-to-metal charge-transfer transitions. On increasing the pH, the growth of a new band at 610 nm was observed, which was accompanied by a color change from pale brown to green and finally to dark brown.

Figure 3a,b shows spectrophotometric data as a function of pH for the chemically prepared osmium(III) complex. Titration data at 610 nm are included in Figure 2. Two stepwise acid–base equilibria were also present in the osmium(III) complex, and pK_{a_3} and pK_{a_4} values of reaction 2 were calculated to be 1.55 ± 0.05

$$[Os^{III}(bpy)_2(BiBzImH_2)]^{3+} \underset{H^+}{\overset{pK_{a_3}}{\rightleftharpoons}}$$
$$[Os^{III}(bpy)_2(BiBzImH)]^{2+} \underset{H^+}{\overset{pK_{a_4}}{\rightleftharpoons}} [Os^{III}(bpy)_2(BiBzIm)]^{+} \quad (2)$$

and 6.40 ± 0.05, respectively. In changing to oxidation state III, pK_a values are decreased by 3.5 ($pK_{a_1} - pK_{a_3}$) and 3.2 ($pK_{a_2} - pK_{a_4}$), respectively. Thus, the protons become considerably more acidic in the higher oxidation state.

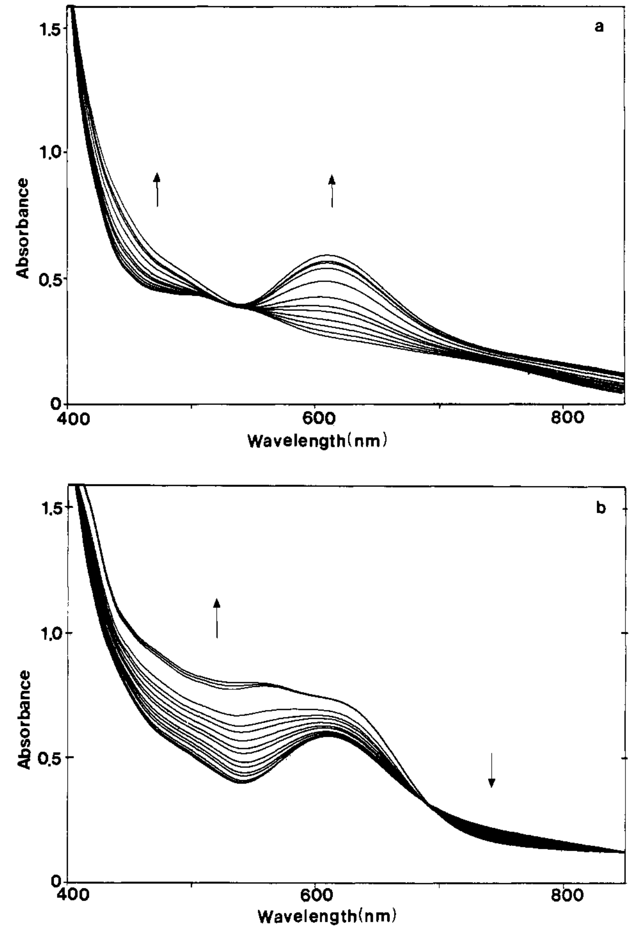

Figure 3. Absorption spectra of $[Os^{III}(bpy)_2(BiBzImH_2)]^{3+}$ (3.14×10^{-4} mol dm^{-3}) at 25 °C generated chemically in CH_3CN/buffer (1:1 v/v) at various pH: (a) lower pH region, pH 0.82, 0.94, 1.05, 1.19, 1.33, 1 44, 1.62, 1.90, 2.23, 2.45, 2.61, and 4.00; (b) higher pH region, pH 4.00, 4.19, 4.33, 4.59, 5.03, 5.16, 5.45, 5.62, 5.89, 5.98, 6.15, 6.32, 6.45, 6.63, 8.85, 9.25, and 9.76.

Electrochemical Studies on the Os(II)/Os(III) Redox Couple. Electrochemical measurements provide information on the difference between two oxidation states. Figure 4 and data in Tables I and II are consistent with a chemically and electrochemically reversible one-electron-oxidation process

$$[Os^{II}(bpy)_2(BiBzImH_2)]^{2+} \rightleftharpoons [Os^{III}(bpy)_2(BiBzImH_2)]^{3+} + e^- \quad (3)$$

accompanied by acid–base equilibria at both glassy-carbon and platinum electrodes. The separation in peak-to-peak potential values, ΔE_p, for oxidation and reduction processes under conditions of cyclic voltammetry are 70 ± 10 mV, and ratios of oxidation to reduction peak height are 1.0 ± 0.1. These data are also similar

Table II. Differential-Pulse Voltammetric Data in CH_3CN/buffer (1:1 v/v) for Oxidation of $[M(bpy)_2(BiBzImH_2)](ClO_4)_2$ at Various pH Values[a]

	M = Ru						M = Os					
	Ru(II)/Ru(III)			Ru(III)/Ru(IV)			Os(II)/Os(III)			Os(III)/Os(IV)		
pH	E^{ox}_p, V vs. Fc/Fc$^+$	$E^r_{1/2}$, V vs. Fc/Fc$^+$	$W_{1/2}$, mV	E^{ox}_p, V vs. Fc/Fc$^+$	$E^r_{1/2}$, V vs. Fc/Fc$^+$	$W_{1/2}$, mV	E^{ox}_p, V vs. Fc/Fc$^+$	$E^r_{1/2}$, V vs. Fc/Fc$^+$	$W_{1/2}$, mV	E^{ox}_p, V vs. Fc/Fc$^+$	$E^r_{1/2}$, V vs. Fc/Fc$^+$	$W_{1/2}$, mV
0.20	+0.704	+0.729	105	+1.260	+1.285	110	+0.260	+0.285	112	+1.290	+1.315	*b*
0.55							+0.256	+0.281	130	+1.236	+1.261	*b*
0.75	+0.696	+0.721	117	+1.192	+1.217	102						
1.12	+0.672	+0.697	115	+1.184	+1.209	133	+0.260	+0.285	113	+1.168	+1.193	*b*
1.50	+0.652	+0.677	103	+1.172	+1.197	128	+0.253	+0.278	107	+1.132	+1.157	*b*
1.85							+0.228	+0.253	113	+1.104	+1.129	*b*
2.10	+0.620	+0.645	110	+1.156	+1.181	117	+0.220	+0.245	102	+1.084	+1.109	120
3.28	+0.560	+0.585	106	+1.076	+1.101	138	+0.156	+0.181	105	+1.012	+1.037	132
3.85	+0.524	+0.549	112	+1.044	+1.069	112	+0.120	+0.145	102	+0.968	+0.993	121
4.40	+0.496	+0.521	109	+1.012	+1.037	112						
4.60							+0.076	+0.101	102	+0.916	+0.941	110
5.30	+0.448	+0.473	122	+0.972	+0.997	119	+0.048	+0.073	105	+0.884	+0.909	119
5.78							+0.024	+0.049	109	+0.853	+0.878	118
5.91	+0.428	+0.453	118	+0.948	+0.973	135						
6.50	+0.404	+0.429	115	+0.924	+0.949	120	+0.004	+0.029	106	+0.844	+0.867	120
7.10	+0.356	+0.381	124	+0.908	+0.933	134	−0.028	−0.003	105	+0.852	+0.877	112
7.70	+0.324	+0.349	115	+0.916	+0.941	*b*						
8.11							−0.084	−0.059	103	+0.848	+0.873	100
8.23	+0.292	+0.317	110	+0.904	+0.929	*b*						
8.48							−0.108	−0.083	96	+0.860	+0.885	*b*
8.90	+0.268	+0.293	115	+0.912	+0.937	*b*						
9.52	+0.224	+0.249	115	*b*	*b*	*b*	−0.164	−0.139	96	*b*	*b*	*b*
9.78							−0.156	−0.131	92	*b*	*b*	*b*
9.98	+0.204	+0.229	114	*b*	*b*	*b*	−0.164	−0.139	102	*b*	*b*	*b*
10.56	+0.184	+0.209	115	*b*	*b*	*b*	−0.168	−0.143	92	*b*	*b*	*b*
11.32	+0.184	+0.209	114	*b*	*b*	*b*	−0.160	−0.135	96	*b*	*b*	*b*
12.65	+0.176	+0.201	109	*b*	*b*	*b*						

[a] glassy-carbon electrode at 25 °C, $W_{1/2}$ = width at half-wave height, pulse height = 50 mV, pulse width = 60 ms, duration between applications of each pulse = 1 s, and scan rate = 4 mV s^{-1}. Other symbols are as in Table I. [b] Ill-defined because of proximity of solvent oxidation.

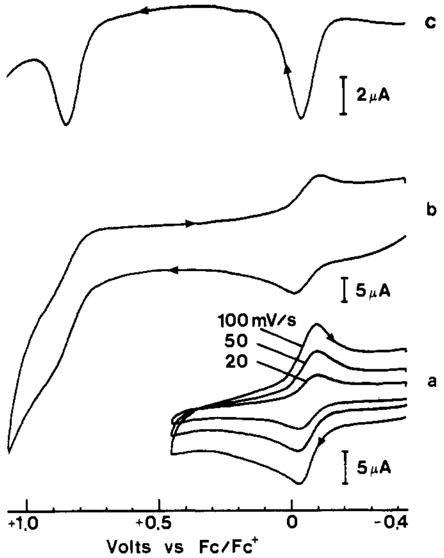

Figure 4. Cyclic voltammograms (a, b) and differential-pulse voltammograms (c) for oxidation of $[Os^{II}(bpy)_2(BiBzImH_2)](ClO_4)_2$ (2×10^{-4} mol dm^{-3}) at a glassy carbon electrode in CH_3CN/H_2O (1:1 v/v) at pH 7.10 and 25 °C. Scan rates are as indicated for curve a and are 100 mV s^{-1} for curve b and 5mV s^{-1} for curve c.

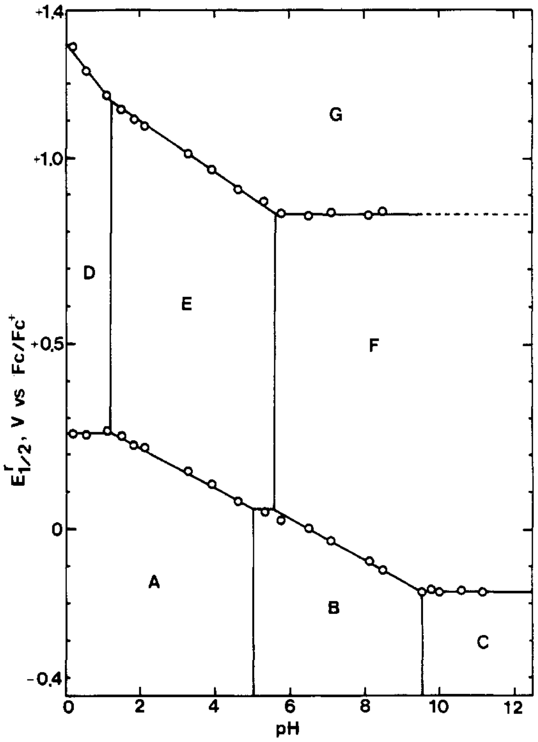

Figure 5. Plots of $E^r_{1/2}$ vs. pH in CH_3CN/buffer (1:1 v/v) for osmium complexes at a glassy-carbon electrode (25 °C): A, $[Os^{II}(bpy)_2(BiBzImH_2)]^{2+}$; B, $[Os^{II}(bpy)_2(BiBzImH)]^+$; C, $[Os^{II}(bpy)_2(BiBzIm)]$; D, $[Os^{III}(bpy)_2(BiBzImH_2)]^{3+}$; E, $[Os^{III}(bpy)_2(BiBzImH)]^{2+}$; F, $[Os^{III}(bpy)_2(BiBzIm)]^+$; G, $[Os^{IV}(bpy)_2(BiBzIm)]^{2+}$.

to that obtained for the known reversible one-electron-oxidation process for ferrocene

$$Fc \rightleftharpoons Fc^+ + e^- \qquad (4)$$

Spectrophotometric data indicate that throughout the pH range studied, three species exist in both oxidation states. At all pH values only one Os(II)/Os(III) wave is observed, which is diffusion controlled. $E^r_{1/2}$ values are pH dependent. If variable-junction potential problems associated with a change in pH have been adequately compensated for via reference to oxidation of ferrocene as an internal standard, then the previously described spectrophotometric results and voltammetric data should be self-consistent with respect to identification of species present in solution. Figure

5 summarizes $E^r_{1/2}$ vs. pH data. Above pH 9.5, $E^r_{1/2}$ is independent of pH and the electrode process is defined as

$$[Os^{II}(bpy)_2(BiBzIm)]^0 \xrightleftharpoons{E^r_{1/2}} [Os^{III}(bpy)_2(BiBzIm)]^+ + e^- \quad (pH > 9.5) \quad (5)$$

where $E^r_{1/2} \approx E° = -0.16$ V vs. Fc/Fc$^+$. At lower pH, acid–base equilibria should be associated with electron transfer, according to spectrophotometric data. In buffered media, equations relating $E^r_{1/2}$ and pH are available.[17] For the general reversible electrode reaction

$$Ox + ne^- + mH^+ \rightleftharpoons Red$$

where Ox = oxidized species and Red = reduced species, the Nernst equation can be readily cast into the form (25 °C)

$$E^r_{1/2} = E°_{298}' - \frac{0.059}{n}(\log (D_{ox}/D_{red})^{1/2}) - 0.059\frac{m}{n}(pH) \quad (6)$$

where $E_{1/2}$ is the half-wave potential, $E°_{298}'$ is the formal electrode potential, and D_{ox} and D_{red} are respectively the diffusion coefficients of Ox and Red. In the derivation of eq 6, it is assumed that the concentration of protons at the electrode surface is equal to that in the bulk solution, which should be true in well-buffered solutions. If the usual assumption $D_{Ox} = D_{Red}$ is applied, then eq 6 can be reduced to

$$E_{1/2} = E°_{298}' - 0.059\frac{m}{n}(pH) \quad (7)$$

Over the pH range 6–9, a plot of $E^r_{1/2}$ vs. pH is linear with a slope of 55.3 mV. This is consistent with a reversible one-proton, one-electron process (eq 8). In the formal sense equations in-

$$[Os^{II}(bpy)_2(BiBzImH)]^+ \rightleftharpoons [Os^{III}(bpy)_2(BiBzIm)]^0 + H^+ + e^- \quad (6 < pH < 9) \quad (8)$$

volving proton content past pH 7 could be written in terms of H_2O/OH^- instead of H^+. However, for simplicity the H^+ format has been retained in eq 8 and elsewhere for all pH values. Extrapolation and location of the intercept with the higher pH-independent region gives a pK_{a_2} value of 9.55 ± 0.05 (see Figure 5), which can be compared with the spectrophotometric value of 9.59 ± 0.05. Results from the two techniques are therefore in excellent agreement. The region pH 4–6 is complex with respect to electrochemical data because of the coexistence of four species: $[Os^{II}(bpy)_2(BiBzImH_2)]^{2+}$, $[Os^{II}(bpy)_2(BiBzImH)]^+$, $[Os^{III}(bpy)_2(BiBzImH)]^{2+}$, and $[Os^{III}(bpy)_2(BiBzIm)]^+$. Furthermore, the difference in pK_a values between oxidation state III and II, $pK_{a_3} - pK_{a_1}$, and $pK_{a_4} - pK_{a_2}$ are almost the same (3.5 and 3.2, respectively). Thus no well-defined discontinuity occurs in the $E_{1/2}$ vs. pH plot.

The slope of the plot of $E^r_{1/2}$ vs. pH over the range 1.5–4.5 is 55.8 mV, against consistent with a one-proton, one-electron reaction (eq 9).

$$[Os^{II}(bpy)_2(BiBzImH_2)]^{2+} \rightleftharpoons [Os^{III}(bpy)_2(BiBzImH)]^{2+} + H^+ + e^- \quad (1.5 < pH < 4.5) \quad (9)$$

At low pH (0–1), $E^r_{1/2}$ is again independent of pH and the electrode process is defined as

$$[Os^{II}(bpy)_2(BiBzImH_2)]^{2+} \rightleftharpoons [Os^{III}(bpy)_2(BiBzImH_2)]^{3+} + e^- \quad (pH < 1) \quad (10)$$

All electrochemical data with respect to the Os(II)/Os(III) process are therefore consistent with spectrophotometric results. Controlled-potential electrolysis of $[Os^{II}(bpy)_2(BiBzImH_2)]^{2+}$ (pH 3.5) at 0.4 V vs. Fc/Fc$^+$ monitored by coulometry gave an n value of 0.99 ± 0.01. The product of electrolysis gave a reversible one-electron reduction step at the same potential as the original oxidation process. Controlled-potential reductive electrolysis at 0.0 V vs. Fc/Fc$^+$ quantitatively regenerates the starting material. The Os(III) complex is apparently very stable and can be also prepared by chemical oxidation with $NOBF_4$ as noted earlier on.

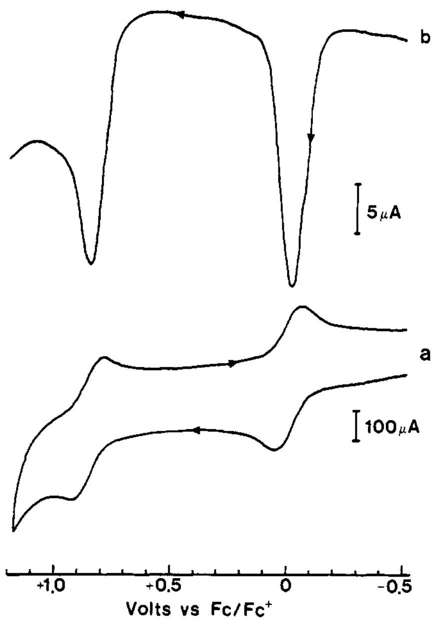

Figure 6. Cyclic voltammogram (a) (scan rate 5 V s^{-1}) and differential-pulse voltammogram (b) (scan rate 4 mV/s, pulse width 60 ms, pulse amplitude 50 mV, 1-s duration between pulse sequences) for oxidation of $[Os(bpy)_2(BiBzImH_2)](ClO_4)_2$ (1×10^{-3} mol dm^{-3}) in CH_3CN/H_2O (1:1 v/v) at pH 7.10 at a glassy-carbon electrode at 25 °C.

Electrochemical Studies of the Os(III)/Os(IV) Couple. The Os(III)/Os(IV) oxidation occurs at very positive potentials and cannot easily be observed at a Pt electrode. Figure 4b shows that under the conditions of cyclic voltammetry at a glassy carbon electrode an irreversible process is observed near the solvent limit. However, the process is well-defined under conditions of differential-pulse voltammetry (Figure 4c). Figure 6a shows that at very fast scan rates (>5 V s^{-1}) the Os(III)/Os(IV) couple is electrochemically reversible. The calculated $E^r_{1/2}$ at pH 7.1 is 0.850 V vs. Fc/Fc$^+$. Figure 6b shows a differential-pulse voltammogram with a pulse amplitude of 50 mV giving a peak potential of 0.836 V vs. Fc/Fc$^+$ (without *iR* correction). After correction for the amplitude term, an $E^r_{1/2}$ value of 0.861 V is obtained. After further correction for *iR* drop, the values from the two techniques agree within experimental error. Thus, the use of *iR*-corrected differential-pulse voltammetric peak potentials accurately reflect the thermodynamic parameter $E^r_{1/2}$ despite the chemical irreversibility of the waves under conditions of cyclic voltammetry at low scan rates.

The independence of $E^r_{1/2}$ on pH over the pH range 6–9 therefore defines the osmium(IV) complex as $[Os^{IV}(bpy)_2(BiBzIm)]^{2+}$, and the electrode process is

$$[Os^{III}(bpy)_2(BiBzIm)]^+ \rightleftharpoons [Os^{IV}(bpy)_2(BiBzIm)]^{2+} + e^- \quad (11)$$

At lower pH, the shift toward more positive potential takes the wave very close to the solvent oxidation limit and data are less precise. However, over the pH range 2–5 the $E^r_{1/2}$ vs. pH plot is linear with a slope of 66 mV, indicative of a one-electron, one-proton step.

$$[Os^{III}(bpy)_2(BiBzImH)]^{2+} \rightleftharpoons [Os^{IV}(bpy)_2(BiBzIm)]^{2+} + H^+ + e^- \quad (12)$$

Over the pH range 0–1 the slope becomes 136 mV, which is consistent with the one-electron, two-proton reaction

$$[Os^{III}(bpy)_2(BiBzImH_2)]^{3+} \rightleftharpoons [Os^{IV}(bpy)_2(BiBzIm)]^{2+} + 2H^+ + e^- \quad (13)$$

The intercept of the two straight lines gives a pK_{a_3} value of 1.25 ± 0.2, which agrees reasonably well with the spectrophotometrically determined value of 1.55 ± 0.05.

The conclusion is that in oxidation state IV only the deprotonated form $[Os(bpy)_2(BiBzIm)]^{2+}$ exists within the 0 < pH <

---

[17] Kolthoff, I. M.; Lingane, J. J. *Polarography*; Interscience: New York, 1952; p 246.

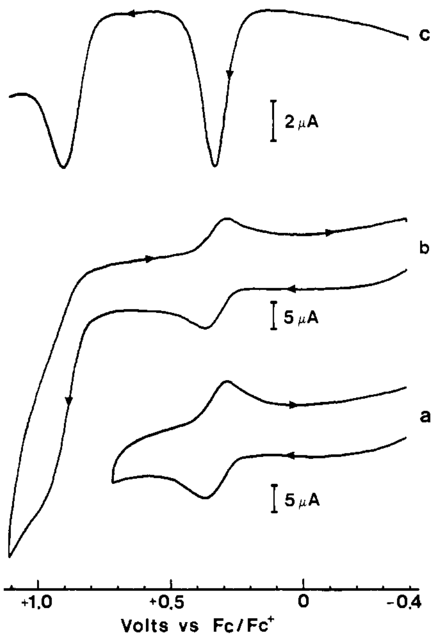

Figure 7. Cyclic voltammograms (a, b) (scan rate 100 mV s^{-1}) and a differential pulse voltammogram (c) (scan rate 5 mV s^{-1}; other parameters as in Figure 6b) for oxidation of $[Ru(bpy)_2(BiBzImH_2)](ClO_4)_2$ (7×10^{-4} mol dm^{-3}) in CH_3CN/H_2O (1:1 v/v) at a glassy-carbon electrode at pH 7.10 and 25 °C.

12 region. The protons in oxidation state IV must be extremely acidic and the pK_a value for the reaction

$$[Os^{IV}(bpy)_2(BiBzImH)]^{3+} \rightleftharpoons [Os^{IV}(bpy)_2(BiBzIm)]^{2+} + H^+ \quad (14)$$

must be <0.

$[Ru(bpy)_2(BiBzImH_2)](ClO_4)_2$. Spectrophotometric Studies of Ruthenium(II). The pK_a values of $[Ru(bpy)_2(BiBzImH_2)](ClO_4)_2$ in 50% aqueous methanol have been already reported.[18] In the 50% acetonitrile/water mixture, the pK_{a_5} and pK_{a_6} values in eq 15 were 5.74 ± 0.05 and 10.51 ± 0.05, which can be compared

$$[Ru(bpy)_2(BiBzImH_2)]^{2+} \underset{H^+}{\overset{pK_{a_5}}{\rightleftharpoons}} [Ru(bpy)_2(BiBzImH)]^+ \underset{H^+}{\overset{pK_{a_6}}{\rightleftharpoons}} [Ru(bpy)_2(BiBzIm)]^0 \quad (15)$$

with the values of 5.7 ± 0.1 and 10.1 ± 0.2 in 50% aqueous methanol.[18] Although the solvent systems of methanol/water and acetonitrile/water are different, similar pK_a values were obtained. Unfortunately, reliable spectrophotometric data for ruthenium(III) complexes could not be obtained with our experimental manipulation procedures because of the high reactivity of ruthenium(III).

Electrochemical Studies of Ru(II)/Ru(III) and Ru(III)/Ru(IV) Couples. Data are summarized in Tables I and II. Figure 7 shows typical cyclic voltammogram and differential-pulse voltammogram of $[Ru(bpy)_2(BiBzImH_2)]^{2+}$ at pH 7.1. Voltammograms show one reversible oxidation couple and one irreversible oxidation wave at more positive potentials. This pattern of voltammetric behavior is almost parallel with that of the osmium analogue, although the peak potentials of ruthenium are shifted to more positive values than those found for osmium. Additionally, at lower pH values the current magnitude for the Ru(III)/Ru(IV) step is considerably larger than that for the Ru(II)/Ru(III) process, which contrasts to the osmium case where the relative values were similar. The potentials for two waves vary with the pH; the $E^r_{1/2}$ vs. pH data are depicted in Figure 8. pK_a values calculated from these data are given in Table III.

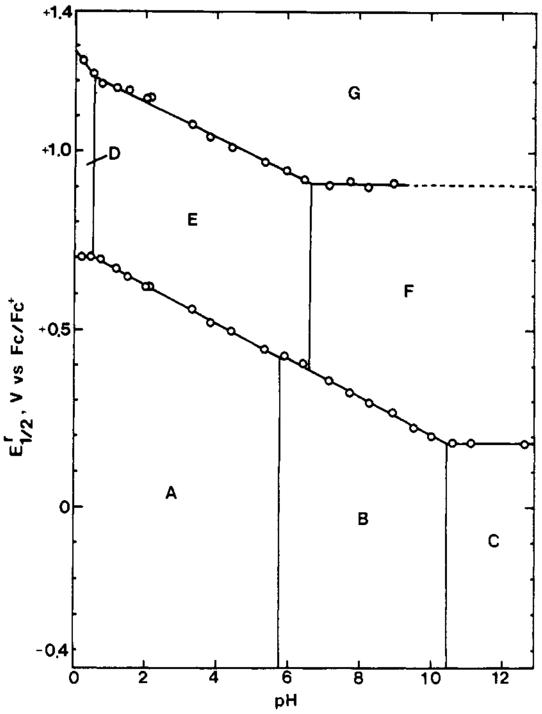

Figure 8. Plots of $E^r_{1/2}$ vs. pH in CH_3CN/buffer (1:1 v/v) for ruthenium complexes at a glassy-carbon electrode (25 °C): A, $[Ru^{II}(bpy)_2(BiBzImH_2)]^{2+}$; B, $[Ru^{II}(bpy)_2(BiBzImH)]^+$; C, $[Ru^{II}(bpy)_2(BiBzIm)]$; D, $[Ru^{III}(bpy)_2(BiBzImH_2)]^{3+}$; E, $[Ru^{III}(bpy)_2(BiBzImH)]^{2+}$; F, $[Ru^{III}(bpy)_2(BiBzIm)]^+$; G, $[Ru^{IV}(bpy)_2(BiBzIm)]^{2+}$.

For the Ru(II)/Ru(III) couple, the potentials are pH independent in the pH <0.6 and >10.4 regions. At these two regions, the major ruthenium(II) species are respectively $[Ru(bpy)_2(BiBzImH_2)]^{2+}$ and $[Ru(bpy)_2(BiBzIm)]$ and the electrode processes are defined as

$$[Ru^{II}(bpy)_2(BiBzImH_2)]^{2+} \rightleftharpoons [Ru^{III}(bpy)_2(BiBzImH_2)]^{3+} + e^- \quad (pH < 0.6) \quad (16)$$

$$[Ru^{II}(bpy)_2(BiBzIm)] \rightleftharpoons [Ru^{III}(bpy)_2(BiBzIm)]^+ + e^- \quad (pH > 10.4) \quad (17)$$

Over the range 0.6 < pH < 5 and 7 < pH < 10 plots of $E^r_{1/2}$ vs. pH are linear with slopes of 53 mV, which are consistent with one-electron, one-proton processes as follows:

$$[Ru^{II}(bpy)_2(BiBzImH_2)]^{2+} \rightleftharpoons [Ru^{III}(bpy)_2(BiBzImH)]^{2+} + H^+ + e^- \quad (0.6 < pH < 5) \quad (18)$$

$$[Ru^{II}(bpy)_2(BiBzImH)]^+ \rightleftharpoons [Ru^{III}(bpy)_2(BiBzIm)]^+ + H^+ + e^- \quad (7 < pH < 10) \quad (19)$$

As for osmium, a clear break point for the two processes was not observed because of the coexistence of four species at intermediate pH values.

For the Ru(III)/Ru(IV) couple, the potentials are pH independent at pH >7 and the electrode reaction is

$$[Ru^{III}(bpy)_2(BiBzIm)]^+ \rightleftharpoons [Ru^{IV}(bpy)_2(BiBzIm)]^{2+} + e^- \quad (pH > 7) \quad (20)$$

At 0.5 < pH < 6, the potentials vary linearly with pH, with a slope of 52 mV, which is indicative of one-electron, one-proton reaction:

$$[Ru^{III}(bpy)_2(BiBzImH)]^{2+} \rightleftharpoons [Ru^{IV}(bpy)_2(BiBzIm)]^{2+} + H^+ + e^- \quad (0.5 < pH < 6) \quad (21)$$

Below pH <0.5, the slope of $E^r_{1/2}$ vs. pH is 124 mV, which is in agreement with the one-electron, two-proton reaction

$$[Ru^{III}(bpy)_2(BiBzImH_2)]^{3+} \rightleftharpoons [Ru^{IV}(bpy)_2(BiBzIm)]^{2+} + 2H^+ + e^- \quad (pH < 0.5) \quad (22)$$

As the solution becomes more acidic than pH 5, the ratio of the Ru(III)/Ru(IV) peak height to that for the Ru(II)/Ru(III)

---

[18] Haga, M. *Inorg. Chim. Acta* **1980**, *45*, L183.

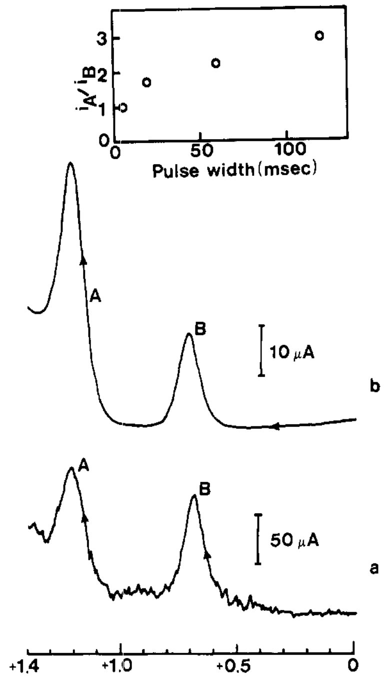

Figure 9. Differential-pulse voltammograms in CH_3CN/H_2O (1:1 v/v) for oxidation of $[Ru(bpy)_2(BiBzImH_2)](ClO_4)_2$ at pH 1.0 using a glassy-carbon electrode (25 °C) at 3 (a) and 60 ms (b) pulse widths, and plot of peak current ratio i_A/i_B vs. pulse width for the second oxidation process (A) and the first oxidation process (B).

process reveals a substantial pulse-width dependence in the differential-pulse voltammetry (Figure 9). At longer pulse widths, the Ru(III)/Ru(IV) peak is much larger than that for the Ru(II)/Ru(III) step. However, both processes Ru(III)/Ru(IV) and Ru(II)/Ru(III) are equal in height with the pulse width <10 ms. These results are consistent with the electrode reaction involving a catalytic reaction, presumably with the solvent (water component) to produce peroxide or oxygen. Equation 23 represents a general form of this class of reaction.

$$[Ru^{III}(bpy)_2(BiBzImH)]^{2+} \rightleftharpoons [Ru^{IV}(bpy)_2(BiBzIm)]^{2+} + H^+ + e^-$$

$$[Ru^{IV}(bpy)_2(BiBzIm)]^{2+} + S_{red} \rightarrow [Ru^{III}(bpy)_2(BiBzImH)]^{2+} + S_{ox}\text{–}H$$

or

$$2[Ru^{IV}(bpy)_2(BiBzIm)]^{2+} + S_{red} \rightarrow 2[Ru^{III}(bpy)_2(BiBzImH)]^{2+} + S_{ox}\text{–}2H \quad (23)$$

Alternative reaction schemes involving a catalytic reaction with the electrolyte (e.g. perchlorate) or oxidative decomposition of the complex would also of course explain the voltammetric data. However, it is clear that the Ru(IV) oxidation state is more reactive in both the thermodynamic and kinetic senses than is Os(IV).

Controlled-potential electrolysis at +0.70 V at pH 7.0 was consistent with a one-electron process to generate Ru(III). However, the product is not nearly as stable as found for the Os(III) analogues, as noted earlier, and appears to be air sensitive. Os complexes in all oxidation states are kinetically inert relative to their ruthenium counterparts.

Comparison between Ru and Os Complexes. Both Ru and Os complexes exhibit similar $E^r_{1/2}$ vs. pH profiles, although potentials and break points are different. For example, the difference in reversible half-wave potentials between M(II)/M(III) and M(III)/M(IV) couples is about 0.53 V for Ru and 0.85 V for Os at pH 4. On the other hand, the potential difference between Ru and Os is about 0.4 V for the M(II)/M(III) couple and but only 0.08 V for the M(III)/M(IV) couple at pH 4. That is, the Os complexes are easier to oxidize than their Ru analogues, although at the III to IV stage differences are not pronounced. The relative ease of oxidation is consistent with the general redox properties of third-row vs. second-row transition-metal complexes.[19]

Table III. pK_a Values Obtained for Coordinated Ligands in Ru and Os Complexes for the Different Oxidation States (25 °C) in CH_3CN/Buffer (1:1 v/v)

complex	pK_a 1st[a]	pK_a 2nd[a]
$[Ru^{II}(bpy)_2(BiBzImH_2)]^{2+}$	5.74	10.51 (10.45)
$[Os^{II}(bpy)_2(BiBzImH_2)]^{2+}$	5.08	9.59 (9.55)
$[Ru^{III}(bpy)_2(BiBzImH_2)]^{3+}$	(0.55)	(6.60)
$[Os^{III}(bpy)_2(BiBzImH_2)]^{3+}$	1.55 (1.25)	6.40 (5.60)
$[Ru^{IV}(bpy)_2(BiBzImH_2)]^{4+}$		(<0)
$[Os^{IV}(bpy)_2(BiBzImH_2)]^{4+}$		(<0)
$[Ru^{II}(bpy)_2(ImH)_2]^{2+}$[b]	11.9	13.3
$[Ru^{III}(NH_3)_5(ImH)]^{3+}$[c]	8.9	
$[Ru^{III}(NH_3)_4(BimH_2)]^{3+}$[d]	5.80 (5.60)	

[a] The values in parentheses were determined electrochemically. Other values were determined spectrophotometrically. [b] Data obtained from ref 20b in ethanol/buffer (1:3 v/v). [c] Data obtained from ref 6f in water. [d] Data obtained from ref 20a in water (phosphate buffer).

Scheme I

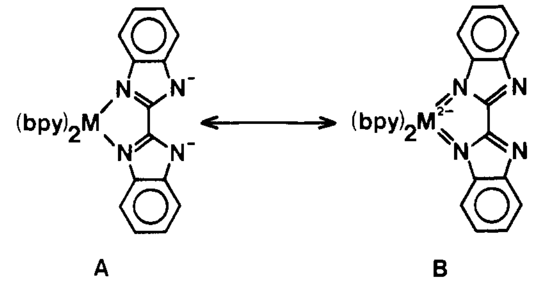

Table III summarizes the pK_a values of Ru and Os complexes in different oxidation states. The pK_a values for related systems are also collected in Table III.[20]

The pK_a for the M(III) oxidation state is about 3–5 pH units higher than that for the M(II) oxidation state (M = Ru, Os). The Ru(III) and Os(III) complexes (d^5 configuration) have better π-acceptor properties than the Ru(II) and Os(II) complexes (d^6 configuration), resulting in greater mixing between the BiBzIm π orbital and the M(III) dπ orbital and enhancing the ease of loss of protons. The ability of the imidazolate ligand to effectively π donate electron density to a low-spin d^5 ion has been recently reported via comparison of pK_a values on the different metal d^n configurations of $[M(NH_3)_5(ImH)]^{3+}$ complexes (M = Ru, Rh, Co, etc.).[5]

In other studies of Ru and Os complexes in higher oxidation states, disproportionation reactions have been reported.[8,10,21] In the present situation the potentials for the $E^r_{1/2}$ vs. pH plots for the M(II)/M(III) and M(III)/M(IV) couples do not cross over at any pH value examined. Thus, disproportionation reactions do not occur, and all oxidation states II, III, and IV are accessible.

Stabilization of Higher Oxidation States by Deprotonation. The potentials of M(III)/M(IV) (M = Ru and Os) couples have been reported for a range of M–bpy complexes: E^{ox}_p = +1.97 V vs. SSCE for the second oxidation process of $Ru(bpy)_2Cl_2$ in CH_3CN,[22] E^{ox}_p = +1.75 V vs. SSCE for $[Ru^{II}(bpy)_2(pz)(pzH)](PF_6)$

---

(19) (a) Pitzer, K. S. *Acc. Chem. Res.* **1979**, *12*, 271. (b) Pyykkö, P.; Desclaux, J. P. *Acc. Chem. Res.* **1979**, *12*, 276. (c) Heath, G. A.; Moock, K. A.; Sharp, D. W. A.; Yellowlees, L. J., *J. Chem. Soc., Chem. Commun.* **1985**, 1503. (d) Taube, H.; *Pure. Appl. Chem.* **1979**, *51*, 901.

(20) (a) Sahai, R.; Murphy, W. R.; Petersen, J. D. *Inorg. Chim. Acta*, in press. (b) Long, C.; Vos, J. G. *Inorg. Chim. Acta* **1984**, *89*, 125.

(21) Takeuchi, K. J.; Thompson, M. S.; Pipes, D. W.; Meyer, T. J. *Inorg. Chem.* **1984**, *23*, 1845.

in CH_3CN (pzH = pyrazole),[22] $E^r_{1/2} = 2.76$ V vs. quasi Ag reference electrode for $[Ru^{II}(bpy)_3](ClO_4)_2$ in SO_2.[23]

In the present case the oxidation potentials of the deprotonated BiBzIm complexes are shifted to considerably more negative potentials compared with those of other complexes, which suggests stronger π-donation of deprotonated BiBzIm to metal stabilizes the higher oxidation states and the contribution of resonance form B becomes larger (Scheme I). The large shift towards a less positive potential enables the oxidation state IV complexes to be observed in aqueous media via oxidation at glassy-carbon electrodes. Recently, the deprotonation of coordinated amide, i.e. amidate nitrogens, has been reported to stabilize the high-valent Pd(IV),[24] Ni(III),[25] Os(VI),[26] and Co(IV).[27] Meyer et al. have reported that loss of protons from aquo ligands on oxidation in $[M(bpy)_2(OH_2)_2]^{2+}$ (M = Ru, Os) complexes results in the stabilization of higher oxidation states, i.e. M(IV), M(V) and M(VI).[21] Naturally, these higher oxidation state species are powerful oxidants. In the present case, reaction with water and/or electrolyte is moderately slow. Reactions of the kind

$$4[M^{IV}(bpy)_2(BiBzIm)]^{2+} + 2H_2O \rightarrow 4[M^{III}(bpy)_2(BiBzImH)]^{2+} + O_2 \quad (24)$$

would explain the catalytic response observed with long time domain voltammetric studies (see also eq 23). This class of reaction has been demonstrated to occur in studies of other Ru(IV) complexes.[28] Catalytic reactions with the sulfur dioxide as the solvent have also been reported.[23]

In this work we have used the formal notation of M(II), M(III), and M(IV) to describe the oxidation processes. However, Bard et al.[29] have suggested that for $[Ru(bpy)_3]^{2+}$ the second oxidation process is ligand based, whereas for $[Os(bpy)_3]^{2+}$ the second oxidation process is assumed to be metal based. In our case, the similarity in pH dependence for both metals leads us to suggest that both oxidation processes are essentially metal based, although of course the concept of formal oxidation states is notoriously treacherous in this area of chemistry.

Acknowledgment. The authors gratefully acknowledge financial support from the Ministry of Education, Japan, and the award of a Gordon Fellowship from the Deakin University Research Committee that made it possible for M.H. to spend a study leave period at Deakin University.

Registry No. $[Os^{II}(bpy)_2(BiBzImH_2)](ClO_4)_2$, 104642-28-6; $[Os^{II}(bpy)_2(BiBzImH_2)]^{2+}$, 104642-27-5; $[Os^{III}(bpy)_2(BiBzImH_2)]^{3+}$, 104642-29-7; $[Os^{II}(bpy)_2(BiBzImH)]^+$, 104642-30-0; $[Os^{II}(bpy)_2(BiBzIm)]$, 104642-31-1; $[Os^{III}(bpy)_2(BiBzImH)]^{2+}$, 104642-32-2; $[Os^{III}(bpy)_2(BiBzIm)]^+$, 104642-33-3; $[Os^{IV}(bpy)_2(BiBzIm)]^{2+}$, 104642-34-4; $[Ru^{II}(bpy)_2(BiBzImH_2)]^{2+}$, 88228-00-6; $[Ru^{II}(bpy)_2(BiBzImH)]^+$, 88437-65-4; $[Ru^{II}(bpy)_2(BiBzIm)]$, 88437-60-9; $[Ru^{III}(bpy)_2(BiBzImH_2)]^{3+}$, 88228-00-6; $[Ru^{III}(bpy)_2(BiBzImH)]^{2+}$, 104642-35-5; $[Ru^{III}(bpy)_2(BiBzIm)]^+$, 104642-36-6; $[Ru^{IV}(bpy)_2(BiBzIm)]^{2+}$, 104642-37-7; $Os(bpy)_2Cl_2$, 15702-72-4; $NOBF_4$, 14635-75-7.

---

(22) Sullivan, B. P.; Salmon, D. J.; Meyer, T. J.; Peedin, J. *Inorg. Chem.* **1979**, *18*, 3369.

(23) Gaudiello, J. G.; Sharp, P. R.; Bard, A. J. *J. Am. Chem. Soc.* **1982**, *104*, 6373.

(24) Hamburg, A.; Ho, C.; Getek, T. A. *Inorg. Chem.* **1985**, *24*, 2593.

(25) Kirksey, S. T.; Neubecker, T. A.; Margerum, D. W. *J. Am. Chem. Soc.* **1979**, *101*, 1631.

(26) Anson, F. C.; Christie, J. A.; Collins, T. J.; Coots, R. J.; Furutani, T. T.; Gipson, S. L.; Keech, J. T.; Kraft, T. E.; Santarsiero, B. D.; Spies, G. H. *J. Am. Chem. Soc.* **1984**, *106*, 4460.

(27) Anson, F. C.; Collins, T. J.; Coots, R. J.; Gipson, S. L.; Richmond, T. G. *J. Am. Chem. Soc.* **1984**, *106*, 5037.

(28) Baar, R. B.; Anson, F. C. *J. Electroanal. Chem.* **1985**, *187*, 265.

(29) Gaudiello, J. G.; Bradley, P. G.; Norton, K. A.; Woodruff, W. H.; Bard, A. J. *Inorg. Chem.* **1984**, *23*, 3.

Contribution from the Department of Chemistry,
University of South Carolina, Columbia, South Carolina 29208

Cluster Syntheses. 13. Chemistry of Sulfidoruthenium Carbonyl Clusters. Synthesis and Characterization of the New Unsaturated Clusters $Ru_4(CO)_{11-n}L_n(\mu_4\text{-}S)_2$ (n = 0–2, L = PMe_2Ph)

Richard D. Adams,* James E. Babin, and Miklos Tasi

Received July 17, 1986

The compound $Ru_3(CO)_9(\mu_3\text{-}CO)(\mu_3\text{-}S)$ (**1**) has been prepared by three methods: pyrolysis and photolysis of $Ru_3(CO)_{10}(\mu\text{-}SPh)(\mu\text{-}H)$, in 89% and 80% yields, respectively, and the reaction of $Ru_3(CO)_{12}$ and ethylene sulfide in 67% yield. The compound $Ru_3(CO)_9(\mu_3\text{-}S)_2$ (**3**) was prepared in 94% yield from the reaction of $Ru_3(CO)_{12}$ with an excess of ethylene sulfide. Compound **3** was also obtained from the reaction of **1** with ethylene sulfide in 97% yield. Compounds **1** and **3** react with hydrogen by loss of CO to form the compounds $Ru_3(CO)_9(\mu_3\text{-}S)(\mu\text{-}H)_2$ (**2**) and $Ru_3(CO)_8(\mu_3\text{-}S)_2(\mu\text{-}H)_2$ (**4**) in 92% and 48% yields, respectively. Compound **4** can be converted back into **3** by reaction with CO under 50 atm pressure in 94% yield. Compound **3** reacts with $Ru(CO)_5$ in the presence of UV irradiation to form the tetraruthenium cluster $Ru_4(CO)_9(\mu\text{-}CO)_2(\mu_4\text{-}S)_2$ (**5**) in 90% yield. The reaction of **4** with PMe_2Ph at 25 °C yields the substitution products $Ru_4(CO)_{11-n}(PMe_2Ph)_n(\mu_4\text{-}S)_2$ (**6**, $n = 1$; **7**, $n = 2$). The structure of **7** was established by a single-crystal X-ray diffraction analysis. Crystal data: space group, $P2_1/n$; $a = 9.752$ (2) Å; $b = 20.471$ (3) Å; $c = 16.236$ (2) Å; $\beta = 93.04$ (1)°; $Z = 4$; $\rho_{calcd} = 2.07$ g/cm^3. The structure was solved by direct methods and was refined (3843 reflections) to the final values of the residuals $R = 0.027$ and $R_w = 0.031$. The molecule consists of a square cluster of four ruthenium atoms with quadruply bridging sulfido ligands on the two square faces of the cluster. Two carbonyl ligands bridge adjacent edges of the square and produce a slight shortening of the two Ru–Ru bonds. The clusters of compounds **5** and **6** are believed to be structurally similar to **7**. Compounds 5–7 contain 62 valence electrons and are therefore electron deficient by two electrons. They do, however, conform to the requirements of the polyhedral skeletal electron pair theory.

Introduction

Sulfur has always played an important role in the chemistry of the transition elements. The sulfido ligand is probably one of the most versatile of all known ligands. It exhibits a wide variety of structural geometries and electron-donating capabilities.[1-4] We have recently synthesized a large number of new sulfidoosmium carbonyl cluster compounds.[5] Some of these possess unusually high reactivities that could have implications for catalysis.[6] The

---

(1) (a) Vahrenkamp, H. *Angew. Chem., Int. Ed. Engl.* **1975**, *14*, 322. (b) Müller, A. *Polyhedron* **1986**, *5*, 323. (c) Abel, E. W.; Crosse, B. C. *Organomet. Chem. Rev.* **1967**, *2*, 443. (d) Coucouvanis, D. *Acc. Chem. Res.* **1981**, *14*, 201.

(2) Adams, R. D.; Foust, D. F. *Organometallics* **1983**, *2*, 323, and references therein.

(3) Adams, R. D.; Hor, R. S. A. *Organometallics* **1984**, *3*, 1915.

(4) Adams, R. D.; Babin, J. E.; Natarajan, K. *J. Am. Chem. Soc.* **1986**, *108*, 3518.

(5) Adams, R. D. *Polyhedron* **1985**, *4*, 2003.

0020-1669/86/1325-4514$01.50/0 © 1986 American Chemical Society